

On the relationship between magnetostatic wave energy and dispersion characteristics in ferrite structures

A V Vashkovsky, E H Lock

DOI: 10.3367/UFNe.0181.201103c.0293

Contents

1. Introduction	281
2. Dispersion relation for a surface magnetostatic wave in a ferrite–dielectric–metal structure	282
3. MSW Poynting vector and power fluxes in a ferrite–dielectric–metal structure	284
4. Variation of MSW dispersion and energy characteristics in a ferrite–dielectric–metal structure	285
5. Whether the magnetostatic approximation can be used in describing the energy characteristics of a magnetostatic wave	287
6. The physical meaning of total and partial power fluxes	289
7. Conclusion	290
References	290

Abstract. The energy and dispersion characteristics of a dipole spin wave in a ferrite–dielectric–metal structure are calculated. An analysis of spin wave dispersion characteristics with extreme points demonstrates how fundamental relationships among the propagation constant, phase and group velocities, Poynting vector, and power flux manifest themselves when the wavenumber changes near these points. A comparison of magnetostatic approximation results with calculations using Maxwell's equations shows the inadequacy of the magnetostatic approximation formulas currently used for calculating the Poynting vector and power flux of dipole spin waves. A correct alternative is proposed.

1. Introduction

Wave processes or waves propagating in various media and structures, while different in nature, have much in common [1, 2]. Thus, the propagation, reflection, and refraction of waves—processes that are all governed by energy and momentum conservation laws—can generally be described within the common physical, terminological, and interpretive framework, and there is a fundamental relationship for any wave between changes of its dispersion and energy characteristics (that is, between the magnitudes and signs of such wave parameters as the propagation constant, phase velocity, group velocity, and electromagnetic energy flux). Generally,

however, it is impossible to find an example of the structure which alone could illustrate all aspects of this relationship, because structures for which the wave dispersion relation exhibits extrema are quite rare in nature (unlike those for which a wave is either forward or backward over its entire range of existence).

One such rare case is illustrated by anisotropic ferrite structures that allow for the effective excitation and subsequent propagation of (electromagnetic type) dipole spin waves, i.e., waves of the ferrite magnetization precession about an external stationary uniform magnetic field [3–6]. In particular, the ferrite–dielectric–metal (FDM) structure has a unique property at certain values of its parameters, which is that the dispersion curve of a dipole spin wave propagating through such a structure has one or two extreme points (see, for example, Refs [7, 8]), providing a convenient example to illustrate all aspects of the interrelation between the dispersion and energy characteristics of the wave.

Because dipole spin waves have phase velocities much less than the speed of light, and so can be treated magnetostatically (i.e., by neglecting terms on the order of about $\partial/\partial t$ in Maxwell's equations), they are standardly referred to as magnetostatic waves (MSWs) [3]. The properties of MSWs have been well studied for a number of structures and are reviewed in detail elsewhere [3–6].

The magnetostatic approximation is a particularly well-suited theoretical framework for MSWs in which the group and phase velocities are noncollinear because, in this case, Maxwell's equations for a medium with the magnetic permeability described by a second-order tensor are rather difficult to solve analytically. Without downplaying the results obtained in the magnetostatic approximation, it should be noted that, because of its unjustified use (even for geometries that can be treated by Maxwell's equations), a number of important fundamental problems have been left virtually unaddressed. Further still, it turned out that the magnetostatic solutions for some of these problems are inadequate for describing the properties and characteristics

A V Vashkovsky, E H Lock V A Kotelnikov Institute of Radio-engineering and Electronics, Fryazino Branch, Russian Academy of Sciences
pl. Vvedenskogo 1, 141190, Fryazino, Moscow region, Russian Federation
Tel. (7-496) 565 25 62. Fax (7-495) 702 95 72
E-mail: edwin@ms.ire.rssi.ru

Received 21 May 2010, revised 25 August 2010
Uspekhi Fizicheskikh Nauk 181 (3) 293–304 (2011)
DOI: 10.3367/UFNr.0181.201103c.0293
Translated by E G Strel'chenko; edited by A Radzig

of dipole spin waves. For example, multiple attempts [5, 6, 9, 10] at calculating the Poynting vector in the magnetostatic approximation (in which the electric component of the superhigh-frequency (SHF) field of an MSW is left out of consideration) have produced expressions which, as shown below, lead to a wrong assessment of MSW energy distribution in some ferrite structures.

In contrast, using Maxwell's equations to examine the characteristics of MSWs — at least for geometries amenable to the analytical solution of the boundary problem — allows the investigation of fluxes, energy distribution, and SHF field lines for an MSW, adding considerable general insight into wave propagation in anisotropic media. In particular, calculations of the MSW Poynting vector and power flux that we perform in this paper for the FDM structure shed light on a question of fundamental importance for wave physics: whether passing through the points of extremum that arise in the MSW dispersion curve for the FDM structure means simultaneous changes in the direction of the wave energy flux and in the character of the wave (the latter meaning a change from a forward to a backward wave or vice versa). While at first glance the answer is obviously positive, calculations with the formulas given in Refs [4, § 5.1], [6, § 6.1], and [9, 10] show it is not. Below, we will also consider reasons why the magnetostatic calculation of MSW energy characteristics leads to incorrect results.

2. Dispersion relation for a surface magnetostatic wave in a ferrite–dielectric–metal structure

As will be seen from the discussion that follows, using Maxwell's equations to examine MSW energy characteristics is most advantageous when dealing with the FDM structure. There has been much work on the derivation of the MSW dispersion relation from Maxwell's equations and on MSW dispersion in various ferrite structures [5, 11–18], so below we only briefly formulate a similar problem for an FDM structure (following mainly Ref. [17]) and present relations necessary to derive expressions for the MSW Poynting vector and power fluxes.

Let us firstly consider MSW propagation through the infinite plane-parallel structure shown in Fig. 1, which consists of a ferrite plate 2 of thickness s , and a nonmagnetic dielectric layer 3 of thickness w adjacent to an ideally conducting metal plane 4. We introduce a Cartesian coordinate system whose associated unit vector triad is $\{\mathbf{x}_0, \mathbf{y}_0, \mathbf{z}_0\}$, and which is oriented in such a way that the x -axis is normal to the plate plane, and the z -axis is along a constant uniform magnetic field \mathbf{H}_0 which magnetizes the plate to saturation. We use the respective notations ϵ_2 and μ_2 for the relative permittivity and the relative permeability tensor of plate 2 and assume the latter to be given by [5]

$$\vec{\mu}_2 = \begin{pmatrix} \mu & iv & 0 \\ -iv & \mu & 0 \\ 0 & 0 & 1 \end{pmatrix}, \quad (1)$$

where

$$\mu = 1 + \frac{\omega_M \omega_H}{\omega_H^2 - \omega^2}, \quad (2)$$

$$v = \frac{\omega_M \omega_H}{\omega_H^2 - \omega^2}, \quad (3)$$

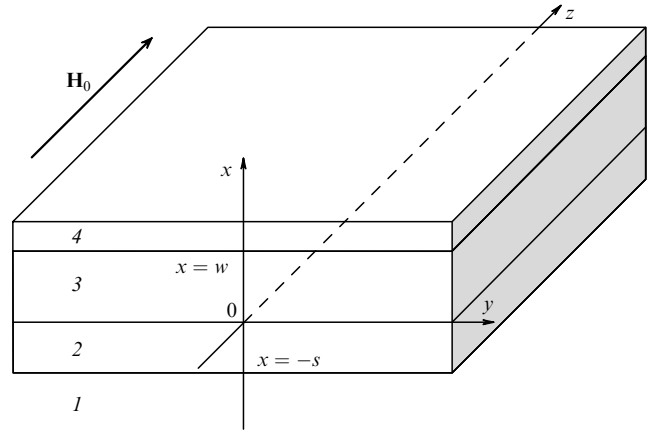


Figure 1. Geometry of the problem: 1, vacuum half-space; 2, ferrite plate; 3, dielectric layer, and 4, perfectly conducting metal.

$\omega_H = \gamma H_0$, $\omega_M = 4\pi\gamma M_0$, $\omega = 2\pi f$, γ is the gyromagnetic constant, $4\pi M_0$ is the ferrite saturation magnetization, and f is the electromagnetic vibration frequency. The relative permittivity of dielectric 3 is ϵ_3 , and the relative permittivity and the relative permeability of the half-space (ϵ_1 and μ_1) are unity, as is the magnetic permeability μ_3 of the dielectric.

The electromagnetic field in each of the media should satisfy Maxwell's equations which, using complex amplitudes [inverse Fourier transforms multiplied by $\exp(i\omega t)$], are as follows:

$$\begin{aligned} \text{rot } \mathbf{h}_j &= i \frac{\omega}{c} \epsilon_j \mathbf{e}_j, \\ \text{rot } \mathbf{e}_j &= -i \frac{\omega}{c} \mu_j \mathbf{h}_j, \\ \text{div}(\epsilon_j \mathbf{e}_j) &= 0, \\ \text{div}(\mu_j \mathbf{h}_j) &= 0, \end{aligned} \quad (4)$$

where \mathbf{h}_j and \mathbf{e}_j are the respective complex amplitudes of the high-frequency magnetic and electric field vectors, ϵ_j and μ_j are the medium parameters (i.e., $j = 1, 2$, or 3), and c is the speed of light in vacuum.

We will be concerned with the wave characteristics along the y -axis, so, assuming the problem to be uniform along the z -axis, we set $\partial/\partial z \equiv 0$ in equations (4). The system (4) then breaks up into two subsystems: the first of these describes TE waves, including MSWs in the structure under study, and the second describes TH waves which will not be considered here (for more detail on TH wave solutions see Ref. [18]). For example, Eqn (4) yields the following set of equations for a TE wave propagating through the ferrite layer:

$$\begin{aligned} \frac{\partial h_{2y}}{\partial x} - \frac{\partial h_{2x}}{\partial y} &= i \frac{\omega}{c} \epsilon_2 e_{2z}, \\ \frac{\partial e_{2z}}{\partial y} &= -i \frac{\omega}{c} (\mu h_{2x} + i v h_{2y}), \\ \frac{\partial e_{2z}}{\partial x} &= i \frac{\omega}{c} (-i v h_{2x} + \mu h_{2y}), \end{aligned} \quad (5)$$

where e_{2z} , h_{2x} , and h_{2y} are the projections of the vectors \mathbf{e}_2 and \mathbf{h}_2 onto the respective coordinate axes. Set of equation (5) is solved for the components e_{2z} of the field and reduced to a Helmholtz wave equation. Equations (4) also readily yield wave equations for the e_{1z} and e_{3z} components in the half-

space and the dielectric. Thus, the e_{jz} field components satisfy the equation

$$\frac{\partial^2 e_{jz}}{\partial x^2} + \frac{\partial^2 e_{jz}}{\partial y^2} + q_j^2 e_{jz} = 0, \quad (6)$$

for each of the media ($j = 1, 2, 3$); here, $q_1^2 = k_0^2$, $q_2^2 = k_0^2 \varepsilon_2 \mu_\perp$, $q_3^2 = k_0^2 \varepsilon_3$, $k_0 = \omega/c$, and $\mu_\perp = (\mu^2 - v^2)/\mu$.

The solutions satisfying equation (6) can be written for each medium as

$$\begin{aligned} e_{1z} &= C \exp(-ik_y y + k_{1x} x), \\ e_{2z} &= \exp(-ik_y y) [A \exp(k_{2x} x) + B \exp(-k_{2x} x)], \\ e_{3z} &= \exp(-ik_y y) [F \exp(k_{3x} x) + G \exp(-k_{3x} x)], \end{aligned} \quad (7)$$

where A, B, C, F, G are arbitrary constants, and the wave vector components k_{jx} and k_y are related by the following equation

$$k_{jx}^2 = k_y^2 - q_j^2. \quad (8)$$

Using system (5) and its analogs for the half-space and the dielectric layer, it is an easy matter to express the magnetic field components h_{jx} and h_{jy} via e_{jz} , and then using Eqn (7) to obtain the following expressions for h_{jx} and h_{jy} :

$$\begin{aligned} h_{1x} &= C \frac{k_y}{k_0} \exp(-ik_y y + k_{1x} x), \\ h_{2x} &= \frac{1}{k_0 \mu_\perp} \left[A \left(k_y - \frac{v}{\mu} k_{2x} \right) \exp(k_{2x} x) \right. \\ &\quad \left. + B \left(k_y + \frac{v}{\mu} k_{2x} \right) \exp(-k_{2x} x) \right] \exp(-ik_y y), \\ h_{3x} &= \frac{k_y}{k_0} [F \exp(k_{3x} x) + G \exp(-k_{3x} x)] \exp(-ik_y y), \\ h_{1y} &= -iC \frac{k_{1x}}{k_0} \exp(-ik_y y + k_{1x} x), \\ h_{2y} &= \frac{i}{k_0 \mu_\perp} \left[A \left(\frac{v}{\mu} k_y - k_{2x} \right) \exp(k_{2x} x) \right. \\ &\quad \left. + B \left(\frac{v}{\mu} k_y + k_{2x} \right) \exp(-k_{2x} x) \right] \exp(-ik_y y), \\ h_{3y} &= i \frac{k_{3x}}{k_0} [G \exp(-k_{3x} x) - F \exp(k_{3x} x)] \exp(-ik_y y). \end{aligned} \quad (9)$$

Satisfying the continuity boundary conditions for the tangential components of the vectors \mathbf{e} and \mathbf{h} at the boundaries $x = -s$ and $x = 0$, and taking the component e_{3z} equal to zero at the metal boundary $x = w$, we arrive at the following system of equations

$$\begin{aligned} C \exp(-k_{1x} s) &= A \exp(-k_{2x} s) + B \exp(k_{2x} s), \\ A + B &= F + G, \\ F \exp(k_{3x} w) + G \exp(-k_{3x} w) &= 0, \\ -k_{1x} \mu_\perp C \exp(-k_{1x} s) &= A \left(\frac{v}{\mu} k_y - k_{2x} \right) \exp(-k_{2x} s) \\ &\quad + B \left(\frac{v}{\mu} k_y + k_{2x} \right) \exp(k_{2x} s), \\ k_{3x} \mu_\perp (G - F) &= A \left(\frac{v}{\mu} k_y - k_{2x} \right) + B \left(\frac{v}{\mu} k_y + k_{2x} \right). \end{aligned} \quad (11)$$

Taking the determinant of the set of equations obtained for the constants A, B, C, F , and G equal to zero yields the following dispersion relation

$$\begin{aligned} &\left(k_{2x} - \frac{v}{\mu} k_y - \mu_\perp k_{1x} \right) \\ &\times \left[\mu_\perp k_{3x} - \left(k_{2x} + \frac{v}{\mu} k_y \right) \tanh(k_{3x} w) \right] \exp(-2k_{2x} s) \\ &+ \left(k_{2x} + \frac{v}{\mu} k_y + \mu_\perp k_{1x} \right) \\ &\times \left[\mu_\perp k_{3x} + \left(k_{2x} - \frac{v}{\mu} k_y \right) \tanh(k_{3x} w) \right] = 0, \end{aligned} \quad (12)$$

which, after some rearrangements, can be rewritten as

$$\begin{aligned} &\left[\mu_\perp^2 k_{1x} k_{3x} + \frac{v^2}{\mu^2} k_y^2 - k_{2x}^2 + \frac{v}{\mu} \mu_\perp k_y (k_{3x} + k_{1x}) \right. \\ &\quad \left. - \mu_\perp k_{2x} (k_{1x} - k_{3x}) \coth(k_{2x} s) \right] \exp(-2k_{3x} w) \\ &+ \mu_\perp^2 k_{1x} k_{3x} - \frac{v^2}{\mu^2} k_y^2 + k_{2x}^2 - \frac{v}{\mu} \mu_\perp k_y (k_{3x} - k_{1x}) \\ &+ \mu_\perp k_{2x} (k_{1x} + k_{3x}) \coth(k_{2x} s) = 0. \end{aligned} \quad (13)$$

If two media 1 and 3 in Fig. 1 may be considered vacuum, then, setting $k_{3x} = k_{1x}$, $\varepsilon_3 = \varepsilon_1 = 1$, and accounting for relationship (8), expression (13) reduces to

$$\begin{aligned} &\left(\mu_\perp k_{1x}^2 - \frac{1}{\mu} k_y^2 + k_0^2 \varepsilon_2 + 2 \frac{v}{\mu} k_y k_{1x} \right) \exp(-2k_{3x} w) \\ &+ \mu_\perp k_{1x}^2 + \frac{1}{\mu} k_y^2 - k_0^2 \varepsilon_2 + 2k_{2x} k_{1x} \coth(k_{2x} s) = 0. \end{aligned} \quad (14)$$

The dispersion relation for a ferrite plate in free space can be obtained from Eqn (14) by assuming $w \rightarrow \infty$ (which leads after simplification to formula (9) of Ref. [18]).

At $w = 0$, i.e., for a ferrite-metal (FM) structure, equation (14) also takes quite a simple form

$$k_{2x} \coth(k_{2x} s) + \frac{v}{\mu} k_y + \mu_\perp k_{1x} = 0. \quad (15)$$

Positive and negative values of k_y in Eqns (12)–(15) correspond to wave propagation in the $+y$ and $-y$ directions, respectively.

All the solutions of equations (12)–(15) may be conditionally classified into two types.

The first describes a wave in which the propagation constant k_y can be several orders of magnitude be greater than k_0 , and for which the smaller the ratio k_0/k_y , the closer the wave dispersion relation to its counterpart calculated magnetostatically (similar to the calculations made in Ref. [18] for a ferrite plate in free space). It is waves corresponding to this solution which we will refer to as MSWs. The second solution is a wave for which k_y is only a few times (depending on the values of ε_2 and ε_3) larger than k_0 (the magnetostatic approximation does not produce such solutions). Surface waves corresponding to this solution are not discussed below because their properties are virtually identical to those of waves arising in an ordinary dielectric plate (see, for example, Ref. [15] for a description of such waves propagating through the FD structure).

It is readily seen that the solutions of equations (12)–(15) may include not only a surface wave, for which k_{2x} and k_{3x} are real and the wave amplitude in the ferrite and dielectric layers is exponential in x , but also bulk wave solutions, for which one of the propagation constants k_{2x} and k_{3x} or simultaneously both become imaginary (this follows from the fact that upon the replacement $k_{3x} \rightarrow ik_{3x}$ in Eqn (12) or $k_{2x} \rightarrow ik_{2x}$ in Eqns (13)–(15), all terms in these equations either remain real or become imaginary). This should be taken into account when deriving the Poynting vector; in particular, writing these expressions in the general form should not be preceded by calculating the real part of the vector product of the electric and magnetic fields.

3. MSW Poynting vector and power fluxes in a ferrite–dielectric–metal structure

As is known, the average value of the Poynting vector (i.e., the time-averaged electromagnetic energy flux density) \mathbf{P} is defined by

$$\mathbf{P} = \frac{c}{8\pi} \operatorname{Re} [\mathbf{e}\mathbf{h}^*], \quad (16)$$

where the symbol $*$ denotes from here on a complex conjugate.

Using expressions (7), (9), (10) for the electromagnetic field components, it can be shown that the only real and nonzero component of the Poynting vector for an MSW in an FDM structure is its y -component:

$$P_{jy} = \frac{c}{8\pi} \operatorname{Re} (e_{jz} h_{jx}^*). \quad (17)$$

Substituting expressions (7) and (9) for the components e_{jz} and h_{jx} into formula (17) yields

$$P_{1y} = \frac{ck_y}{8\pi k_0} |C|^2 \exp(2k_{1x}x), \quad (18)$$

$$P_{2y} = \frac{c}{8\pi k_0 \mu_{\perp}} \operatorname{Re} \left[|A|^2 \left(k_y - \frac{v}{\mu} k_{2x} \right) \exp(2k_{2x}x) + |B|^2 \left(k_y + \frac{v}{\mu} k_{2x} \right) \exp(-2k_{2x}x) + AB^* \left(k_y + \frac{v}{\mu} k_{2x} \right) + BA^* \left(k_y - \frac{v}{\mu} k_{2x} \right) \right], \quad (19)$$

$$P_{3y} = \frac{ck_y}{8\pi k_0} \operatorname{Re} [|F|^2 \exp(2k_{3x}x) + |G|^2 \exp(-2k_{3x}x) + FG^* + GF^*]. \quad (20)$$

Using system (11), relations (18)–(20) for the Poynting vector components and relations (7), (9), (10) for the SHF field components can be expressed in terms of (any) one of the five independent coefficients A, B, C, F, G . For this purpose, let us express, for example, B, C, F, G in terms of A :

$$\begin{aligned} B &= A\xi \exp(-2k_{2x}s), \\ C &= A(\xi + 1) \exp(k_{1x}s - k_{2x}s), \\ G &= A\beta, \\ F &= -G \exp(-2k_{3x}w) = -A\beta \exp(-2k_{3x}w) = A\eta, \end{aligned} \quad (21)$$

where

$$\xi = \frac{k_{2x} - (v/\mu)k_y - \mu_{\perp}k_{1x}}{k_{2x} + (v/\mu)k_y + \mu_{\perp}k_{1x}}, \quad (22)$$

$$\eta = \frac{1 + \xi \exp(-2k_{2x}s)}{1 - \exp(2k_{3x}w)}, \quad (23)$$

$$\beta = \frac{1 + \xi \exp(-2k_{2x}s)}{1 - \exp(-2k_{3x}w)}. \quad (24)$$

As calculations showed, for MSW type solutions the components k_{2x} and k_{3x} are real for $k_y \gg k_0$, whereas the components k_{2x} and k_{3x} become imaginary for k_y close to k_0 (a similar change in k_{2x} and k_{3x} for the FD structure is shown in Fig. 3 in Ref. [15]), with the result that ξ, η, β , the coefficients B, C, F, G , and all field components e_{jz}, h_{jx}, h_{jy} become complex. Therefore, relations (18)–(20) for different ranges of k_y values produce different expressions for the y -components of the Poynting vector and corresponding power fluxes. Because our concern here is with the energy characteristics of MSWs, for which $k_y \gg k_0$, the components k_{2x} and k_{3x} , the quantities ξ, η, β , and the coefficients B, C, F, G are real, so that from expressions (18)–(20), using formulas (21), the MSW Poynting vector components are given by

$$P_{1y} = P_{0y}(\xi + 1)^2 \exp[-2k_{2x}s + 2k_{1x}(x + s)], \quad (25)$$

$$P_{2y} = \frac{P_{0y}}{\mu_{\perp}} \exp(-2k_{2x}s) \left\{ \left(1 - \frac{vk_{2x}}{\mu k_y} \right) \exp[2k_{2x}(x + s)] + \xi^2 \left(1 + \frac{vk_{2x}}{\mu k_y} \right) \exp[-2k_{2x}(x + s)] + 2\xi \right\}, \quad (26)$$

$$\begin{aligned} P_{3y} &= P_{0y} [\eta^2 \exp(2k_{3x}x) + \beta^2 \exp(-2k_{3x}x) + 2\beta\eta] \\ &= P_{0y} [\eta \exp(k_{3x}x) + \beta \exp(-k_{3x}x)]^2, \end{aligned} \quad (27)$$

where

$$P_{0y} = \frac{ck_y |A|^2}{8\pi k_0}. \quad (28)$$

The total MSW power flux Π will be the sum of power flux contributions Π_j from all media ($j = 1, 2, 3$), each of which is obtained by integrating the corresponding y -components of the Poynting vector P_{jy} over the x and z coordinates:

$$\begin{aligned} \Pi &= \sum_{j=1}^3 \Pi_j = \int_0^1 \int_{-\infty}^{-s} P_{1y} dx dz \\ &+ \int_0^1 \int_{-s}^0 P_{2y} dx dz + \int_0^1 \int_0^w P_{3y} dx dz. \end{aligned} \quad (29)$$

Because the structure under study is uniform along the z -axis, the integration with respect to z is formal and reduces to multiplying by the length of a unit region, whereas Π_j has the meaning¹ of the power flux through the j th medium along the y -axis per unit length of the structure along the z -axis. Substituting expressions (25)–(27) for the y -component P_{jy} of the Poynting vector into formula (29) and performing integration, we obtain the following expression for the partial

¹ The physical meaning of a partial flow Π_j is defined more precisely in Section 6.

flux Π_j ($j = 1, 2, 3$):

$$\Pi_1 = \frac{P_{0y} \exp(-2k_{2x}s)}{2k_{1x}} (\xi + 1)^2, \quad (30)$$

$$\Pi_2 = \frac{P_{0y} \exp(-2k_{2x}s)}{2k_{2x}\mu_{\perp}} \left\{ \left(1 - \frac{vk_{2x}}{\mu k_y} \right) [\exp(2k_{2x}s) - 1] + \xi^2 \left(1 + \frac{vk_{2x}}{\mu k_y} \right) [1 - \exp(-2k_{2x}s)] + 4\xi k_{2x}s \right\}, \quad (31)$$

$$\begin{aligned} \Pi_3 &= \frac{P_{0y}}{2k_{3x}} \left\{ \eta^2 [\exp(2k_{3x}w) - 1] + \beta^2 [1 - \exp(-2k_{3x}w)] + 4\beta\eta k_{3x}w \right\} \\ &= \frac{P_{0y}\beta^2 \exp(-2k_{3x}w)}{2k_{3x}} \\ &\quad \times [\exp(2k_{3x}w) - \exp(-2k_{3x}w) - 4k_{3x}w]. \end{aligned} \quad (32)$$

4. Variation of MSW dispersion and energy characteristics in a ferrite–dielectric–metal structure

There is a fundamental relationship that characterizes changes in the dispersion and energy characteristics of any wave and which is particularly manifested in the propagation of a surface MSW (SMSW) in an FDM structure. As is known, this structure exhibits a unique feature in that its dispersion curve may have one or two points of extremum (where the derivative $\partial\omega/\partial k_y$ changes sign), indicating that the wave changes its character at these points (from a forward wave for one range of values of the propagation constant k_y to a backward wave for another). At the same time, it is known that for the same sign of k_y , forward and backward waves should carry energy in opposite directions—that is, depending on the character of the wave, the total energy flux will have different signs in intervals of the values of k_y separated by the points of extremum. The theoretical and experimental confirmation of this relationship between wave dispersion and energy characteristics is of fundamental significance for the physics of waves.

Let us now consider how the dispersion and energy characteristics of an SMSW in the FDM structure vary with the parameters of the latter. We will simplify our calculations by assuming that the dielectric layer 3 in the FDM structure displayed in Fig. 1 is a vacuum gap ($\epsilon_3 = 1$), and plate 2 is yttrium iron garnet (YIG), a ferrite which is most effective in exciting and propagating MSWs. For a YIG plate of thickness $s = 10 \mu\text{m}$, a saturation magnetization $4\pi M_0 = 1750 \text{ G}$, and an external magnetic field $H_0 = 300 \text{ Oe}$, the dispersion curve $f(k_y)$ for an SMSW in an FDM structure varies with vacuum gap w as shown in Fig. 2. Curves $f(k_y)$ for an FDM structure always lie between curve 1, the SMSW dispersion curve for the FM structure (which corresponds to $w = 0$), and curve 4, the SMSW dispersion curve for a ferrite plate in free space (which corresponds to $w \rightarrow \infty$), and have the feature that for the range $0 < w < w_1$ the function $f(k_y)$ has a single point of extremum (see Fig. 2, curve 2), for the range $w_1 < w < w_2$ it has two points of extremum (see Fig. 2, curve 3), and for $w_2 < w < \infty$ it has no extrema [$f(k_y)$ for this case is not plotted in Fig. 2].

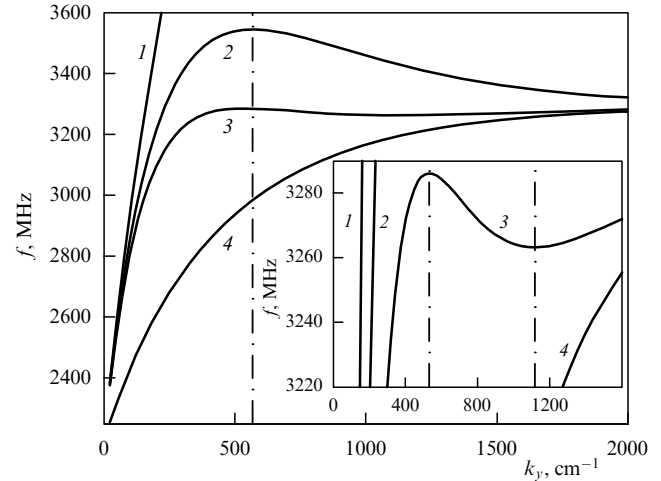


Figure 2. MSW dispersion curves $f(k_y)$ for an FDM structure for different vacuum gaps: 1, $w = 0$ (i.e., FM structure); 2, $w = 10 \mu\text{m}$; 3, $w = 15.5 \mu\text{m}$, and 4, $w \rightarrow \infty$ (i.e., ferrite plate in a free space). Vertical dashed-dot lines mark the values of k_y at which $f(k_y)$ has extrema.

The variation of the total and partial fluxes calculated by formulas (29)–(32) is shown in Fig. 3 for the case (Fig. 3a) in which the dispersion curve $f(k_y)$ for an FDM structure has a single extremum and is described by curve 2 in Fig. 2, and for the case (Fig. 3b) in which this curve shows two points of extremum and is described by curve 3 in Fig. 2.

As seen from Fig. 3, the total flux Π behaves in exact correspondence with how its associated dispersion relation does: for those k_y where $f(k_y)$ has extrema, $\Pi(k_y)$ passes through zero, with the total flux Π and the wave propagation constant k_y (phase velocity) having the same sign for those ranges of k_y values where the wave is forward (i.e., where the dot product of the wave vector and the group velocity has a positive sign, $\mathbf{k}_y \mathbf{V} = \mathbf{k}_y \partial\omega/\partial \mathbf{k}_y > 0$ [19, 20]); on the other hand, for those ranges of k_y values where the wave is backward ($\mathbf{k}_y \mathbf{V} = \mathbf{k}_y \partial\omega/\partial \mathbf{k}_y < 0$), the total flux Π and the wave propagation constant k_y (phase velocity) have the opposite signs.² In cases where the dispersion curve has no extrema and describes a forward wave [as is the case for dependences $f(k_y)$ described by curves 1 and 4 in Fig. 2], the total flux Π is always positive (flux changes corresponding to these dispersion curves are not shown in Fig. 3). This relationship between the dispersion and energy characteristics is a fundamental property which characterizes the propagation not only of an MSW in an FDM structure, but also of any electromagnetic waves in anisotropic or dielectric media. While there has been considerable theoretical work on the propagation of MSWs in an FDM [7–13], no investigation of this relationship has been undertaken.

It should be noted that of the three terms Π_1 , Π_2 , and Π_3 that determine the total flux Π , fluxes Π_1 and Π_3 in vacuum always have the same sign as the propagation constant k_y , which, in accordance with Eqn (28), determines the sign of the amplitude of the MSW energy characteristics P_{0y} (i.e., if $k_y > 0$, then $\Pi_1 > 0$ and $\Pi_3 > 0$). However, the flux Π_2 in the ferrite layer changes its sign in a more complicated way: at $w = 0$, Π_2 and k_y have the same sign; as $w \rightarrow \infty$, Π_2 and k_y have opposite signs, and for intermediate gap widths w , Π_2

² The formulation given is general and takes into account the fact that in a number of structures dispersion curves have extreme points at negative k_y .

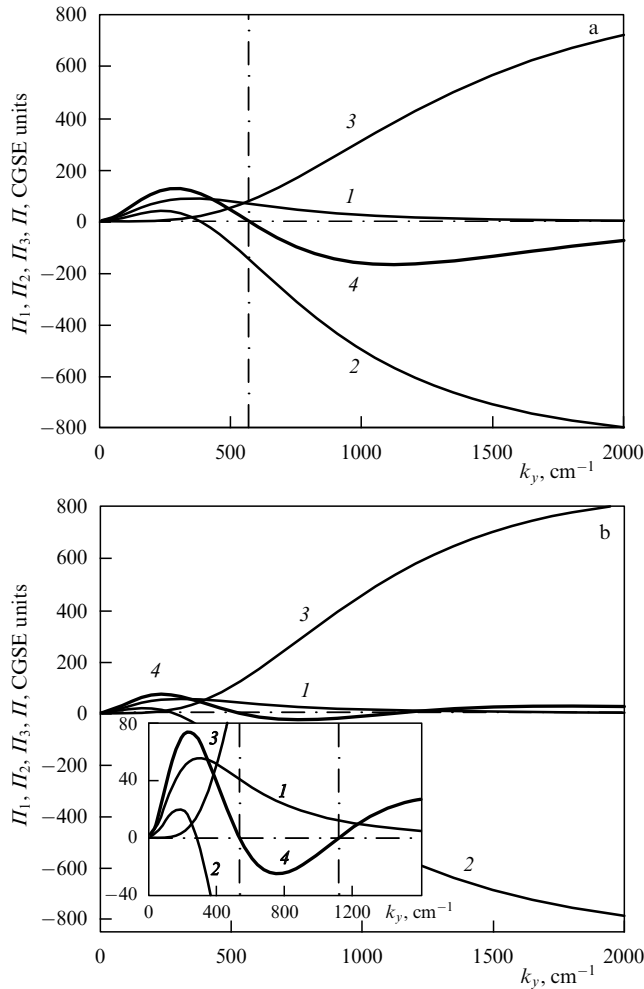


Figure 3. Total and partial MSW power fluxes in an FDM structure as a function of the MSW propagation constant k_y for $w = 10 \mu\text{m}$ (a) and $w = 15.5 \mu\text{m}$ (b): 1, Π_1 in the vacuum half-space; 2, Π_2 in the ferrite layer; 3, Π_3 in the vacuum gap; 4, total flux Π in the structure. Horizontal dashed-dot lines mark the value of $\Pi = 0$; vertical lines mark k_y values for which $\Pi = 0$.

can have either positive or negative sign depending on where k_y is.³ We recall here that the negative values of a partial flux appearing in one of the layers of the structure are characteristic not only of a ferrite layer but also of, for example, a plasma layer, as shown in Ref. [21].

To better understand the physics behind the above-described variation of the total and partial fluxes, let us consider how the Poynting vector P_y and its determinant superhigh-frequency electric and magnetic fields e_z and h_x vary over the cross section of the structure. The normalized $P_y(x)$, $e_z(x)$, and $h_x(x)$ dependences calculated from formulas (7), (9), (25)–(27) at the frequency $f = 3100 \text{ MHz}$ are shown in Fig. 4. In a free ($w \rightarrow \infty$) ferrite plate, the wave is localized near one of the plate's surfaces (Fig. 4a), where all three quantities P_y , e_z , and h_x have maxima. As this surface is approached sufficiently closely by a metal plane (to within about a few ferrite plate thicknesses), the maxima of the SHF field e_z and the values of P_y steadily shift toward the opposite

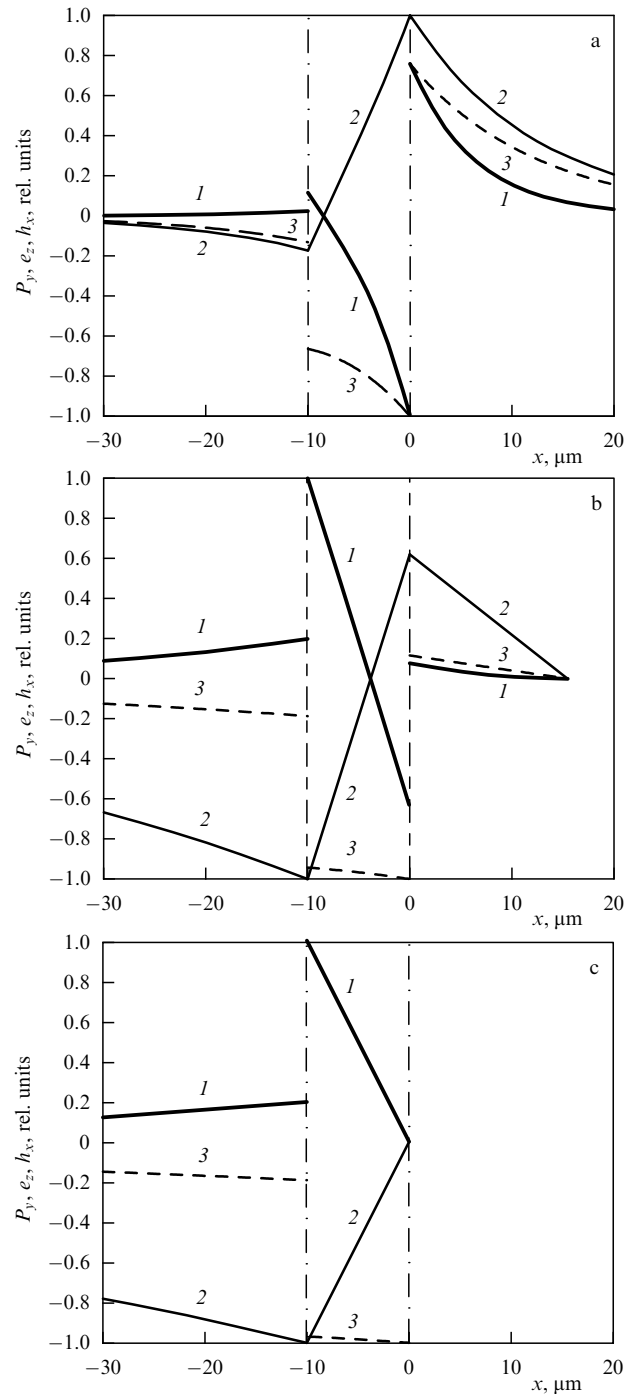


Figure 4. Variation of the time-averaged electromagnetic energy flux density P_y (1) and SHF components of the electric field e_z (2) and magnetic field h_x (3) along an FDM structure cross section at $f_0 = 3100 \text{ MHz}$ for different vacuum gap widths: (a) $w \rightarrow \infty$ (ferrite plate in a free space), (b) $w = 15.5 \mu\text{m}$, (c) $w = 0$ (FM structure). Vertical dashed-dot lines correspond to the lower and upper surfaces of the ferrite plate. Maxwell's equations and formula (16) were used in the calculations.

surface (Fig. 4b) because, as is known, on an ideally conducting surface $e_z = 0$ (and hence $P_y = 0$). If the metal plane is adjacent to the surface of the ferrite plate (at $w = 0$), e_z and P_y are zero here, and have their maxima near the opposite surface. The quantities e_z and P_y behave in this way not only for $f = \text{const}$ but for $k_y = \text{const}$, as well. As for the properties of the wave itself, the factors determining whether the wave will be forward or backward for the given structure

³ It should be recalled that all the mentioned properties of the Π_1 , Π_2 , and Π_3 fluxes are characteristic of an MSW, i.e., of those values of k_y for which the components k_{2x} and k_{3x} are real.

peculiarities, frequency, and the value of k_y are the parameters of the exponential functions that describe P_y : the total area under the curve $P_y(x)$ in Fig. 4 (i.e., the flux Π) will be positive (the forward wave) or negative (the backward wave) depending on how sharply or smoothly the exponentials fall off.

Importantly for the subject under discussion, the results described above received experimental support from an earlier work [17]. This work proved that there is a relationship between the energy and dispersion characteristics of an MSW in an FDM structure: not only were forward and backward MSWs corresponding to the rising and falling portions of the dispersion curve observed in this work, but it was also shown how using the variation in the phase-frequency characteristic of the transmission coefficient can help to distinguish a forward from a backward wave. Reference [17] was also able to investigate MSW characteristics in an FDM structure by using a YIG plate with a dielectric and a metal screen located at one side, and an exciting and a receiving transducer at the other (such measurements were not possible for YIG films because one side of a YIG film is adjacent to the substrate on which the film was grown).

5. Whether the magnetostatic approximation can be used in describing the energy characteristics of a magnetostatic wave

It might seem on the first glance that the results described above are, first, trivial and unquestionable, and, second, simpler to obtain in the magnetostatic approximation (as Refs [4, § 5.1], [6, § 6.1], and [9, 10] suggest).

We will show below what errors arise when using the magnetostatic approximation to study the energy characteristics of an MSW. For this purpose, we will try to use magnetostatic calculations to obtain dependences similar to those plotted in Figs 3 and 4.

Let us solve a boundary value problem for the FDM structure of Fig. 1 using Maxwell's equations in the magnetostatic approximation:

$$\text{rot } \mathbf{h} = 0, \quad (33)$$

$$\text{div } \mathbf{b} = 0. \quad (34)$$

Introducing the magnetostatic potential Ψ for each medium ($j = 1, 2, 3$), so that

$$\mathbf{h}_j = \text{grad } \Psi_j, \quad (35)$$

and using the respective expressions $\mathbf{b}_2 = \vec{\mu}_2 \mathbf{h}_2$ and $\mathbf{b}_{1,3} = \mathbf{h}_{1,3}$ for magnetic induction inside and outside the ferrite plate, we obtain the following equations for the potential inside (Ψ_2) and outside ($\Psi_{1,3}$) the plate:

$$\mu \left(\frac{\partial^2 \Psi_2}{\partial x^2} + \frac{\partial^2 \Psi_2}{\partial y^2} \right) + \frac{\partial^2 \Psi_2}{\partial z^2} = 0, \quad (36)$$

$$\frac{\partial^2 \Psi_{1,3}}{\partial x^2} + \frac{\partial^2 \Psi_{1,3}}{\partial y^2} + \frac{\partial^2 \Psi_{1,3}}{\partial z^2} = 0. \quad (37)$$

The continuity of the potential Ψ and of the normal component b_x of the magnetic induction at the interfaces, combined with the requirement that this component vanish at the surface of the metal, leads to the following boundary

conditions:

$$\begin{aligned} \Psi_1 &= \Psi_2 \quad \text{at } x = -s, \\ \Psi_2 &= \Psi_3 \quad \text{at } x = 0, \\ \frac{\partial \Psi_3}{\partial x} &= 0 \quad \text{at } x = w, \\ \mu \frac{\partial \Psi_2}{\partial x} + i\nu \frac{\partial \Psi_2}{\partial y} &= \frac{\partial \Psi_1}{\partial x} \quad \text{at } x = -s, \\ \mu \frac{\partial \Psi_2}{\partial x} + i\nu \frac{\partial \Psi_2}{\partial y} &= \frac{\partial \Psi_3}{\partial x} \quad \text{at } x = 0. \end{aligned} \quad (38)$$

We assume for each of the media the following form for the solution which describes an MSW propagation in the plane of the structure and satisfies Eqns (36) and (37):

$$\begin{aligned} \Psi_1 &= C \exp(-ik_y y - ik_z z + k_{1x} x), \\ \Psi_2 &= \exp(-ik_y y - ik_z z) [A \exp(k_{2x} x) + B \exp(-k_{2x} x)], \\ \Psi_3 &= \exp(-ik_y y - ik_z z) [F \exp(k_{3x} x) + G \exp(-k_{3x} x)], \end{aligned} \quad (39)$$

where A, B, C, F , and G are arbitrary constants, and $k_{1x}, k_{2x}, k_{3x}, k_y$, and k_z are wave vector components along the coordinate axes (of which k_{1x}, k_{2x} , and k_{3x} are positive). By substituting expressions (39) into Eqns (36) and (37), the relationships between the wave vector components are found to be

$$\begin{aligned} k_{1x} &= \sqrt{k_y^2 + k_z^2}, \\ k_{2x} &= \sqrt{k_y^2 + \frac{k_z^2}{\mu}}, \\ k_{3x} &= k_{1x}. \end{aligned} \quad (40)$$

Substituting expressions (39) into Eqn (38), we obtain the system of equations

$$\begin{aligned} C \exp(-k_{1x} s) &= A \exp(-k_{2x} s) + B \exp(k_{2x} s), \\ A + B &= F + G, \\ F \exp(k_{3x} w) - G \exp(-k_{3x} w) &= 0, \\ \frac{k_{1x}}{\mu} C \exp(-k_{1x} s) &= A \left(\frac{\nu}{\mu} k_y + k_{2x} \right) \exp(-k_{2x} s) \\ &\quad + B \left(\frac{\nu}{\mu} k_y - k_{2x} \right) \exp(k_{2x} s), \\ \frac{k_{3x}}{\mu} (F - G) &= A \left(\frac{\nu}{\mu} k_y + k_{2x} \right) + B \left(\frac{\nu}{\mu} k_y - k_{2x} \right), \end{aligned} \quad (41)$$

which, when solved, yields the following dispersion relation (see, for example, a table in Ref. [22]) for MSW propagation in an FDM structure:

$$\begin{aligned} \mu^2 k_{2x}^2 - \nu^2 k_y^2 + k_{1x}^2 + 2\mu k_{1x} k_{2x} \coth(k_{2x} s) \\ + (\mu^2 k_{2x}^2 - \nu^2 k_y^2 - k_{1x}^2 + 2\nu k_{1x} k_y) \exp(-2k_{1x} w) &= 0. \end{aligned} \quad (42)$$

Assuming wave propagation along the y -axis (to make the problem similar to that of Sections 2–4) and setting $k_z = 0$, equation (42) can be written out using formulas (40) as

$$\mu_{\perp} + \frac{1}{\mu} + 2 \coth(k_y s) + \left(\mu_{\perp} - \frac{1}{\mu} + 2 \frac{\nu}{\mu} \right) \exp(-2k_y w) = 0. \quad (43)$$

To describe the energy characteristics of an MSW in the magnetostatic approximation, the proposal to use the well-known vector analysis identity

$$\operatorname{div}[\mathbf{e}\mathbf{h}^*] = \mathbf{h}^* \operatorname{rot} \mathbf{e} + \mathbf{e} \operatorname{rot} \mathbf{h}^* \quad (44)$$

has been made [4, § 5.1], [6, § 6.1], and [9, 10]. Because $\operatorname{rot} \mathbf{h} = 0$, $\operatorname{rot} \mathbf{e} = -ik_0 \mathbf{b}$, and $\mathbf{h} = \operatorname{grad} \Psi$ [see Eqns (33), (4), and (35), respectively], identity (44) yields

$$\operatorname{div}[\mathbf{e}\mathbf{h}^*] = -ik_0 \mathbf{h}^* \mathbf{b} = -ik_0 \operatorname{grad} \Psi^* \mathbf{b}. \quad (45)$$

Bearing in mind that $\operatorname{div} \mathbf{b} = 0$ [see Eqn (34)], Eqn (45) can be rewritten as

$$\operatorname{div}[\mathbf{e}\mathbf{h}^*] = -ik_0 \operatorname{div}(\Psi^* \mathbf{b}), \quad (46)$$

which, in accordance with the conclusions of Refs [4, § 5.1], [6, § 6.1], and [9, 10], implies that

$$[\mathbf{e}\mathbf{h}^*] = -ik_0 \Psi^* \mathbf{b}, \quad (47)$$

meaning that the Poynting vector (16) for each of the media ($j = 1, 2, 3$) can be written out as

$$\mathbf{P}_j = -\frac{\omega}{8\pi} \operatorname{Re}(i\Psi_j^* \mathbf{b}_j). \quad (48)$$

The immediate point here is that the passage from Eqn (46) to Eqn (47) is incorrect because two vectors can be different even if they have the same divergence (as is obviously the case for the vectors $x\mathbf{x}_0 + y\mathbf{y}_0 + z\mathbf{z}_0$ and $5x\mathbf{x}_0 - 4y\mathbf{y}_0 + 2z\mathbf{z}_0$). Using the exponential functions describing the coordinate dependences of the vectors \mathbf{e} and \mathbf{h} , it is an easy matter to construct an example of such vectors:

$$\begin{aligned} & \frac{1}{k_x} \exp(k_x x - ik_y y - ik_z z) \mathbf{x}_0 \\ & + \frac{1}{ik_y} \exp(k_x x - ik_y y - ik_z z) \mathbf{y}_0 \\ & + \frac{1}{ik_z} \exp(k_x x - ik_y y - ik_z z) \mathbf{z}_0, \\ & \frac{2}{k_x} \exp(k_x x - ik_y y - ik_z z) \mathbf{x}_0 \\ & - \frac{4}{ik_y} \exp(k_x x - ik_y y - ik_z z) \mathbf{y}_0 \\ & + \frac{7}{ik_z} \exp(k_x x - ik_y y - ik_z z) \mathbf{z}_0. \end{aligned}$$

We thus see that formula (48) obtained from formula (47) is also incorrect.

Let us, however, forget this error for a while and look at what the calculations using formula (48) yield. Notice that in the case of the y -propagating MSW we are considering, the only Poynting vector component which takes real values is $P_{jy} = -\omega \operatorname{Re}(i\Psi_j^* b_{jy})/8\pi$. Figure 5 shows the results obtained from formula (48) for the normalized dependences $\Psi(x)$, $b_y(x)$, and $P_y(x)$ for a ferrite plate in a free space ($w \rightarrow \infty$) (Fig. 5a) and for the FM structure ($w = 0$) (Fig. 5b), all produced for the same media parameters used in calculations with Maxwell's equations in Section 4.⁴ Comparing Figs 4c

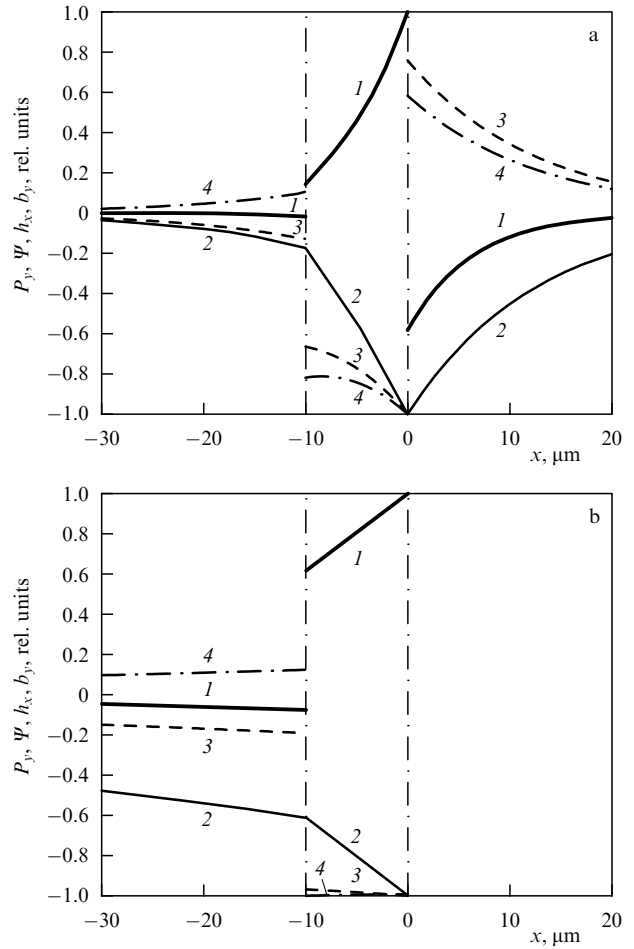


Figure 5. Variation of the time-averaged electromagnetic energy flux density P_y (1), magnetic potential Ψ (2) and SHF magnetic field components h_x (3) and magnetic induction b_y (4) along an FDM structure cross section at $f_0 = 3100$ MHz for different vacuum gap widths: (a) $w \rightarrow \infty$ (ferrite plate in a free space), and (b) $w = 0$ (FM structure). Vertical dashed-dotted lines correspond to the lower and upper surfaces of the ferrite plate. Calculations were done using formula (48) in the text.

and 5b, it is seen that, unlike $P_y(x)$ calculated for an FM structure using Maxwell's equations (Fig. 4c, curve 1), the similar $P_y(x)$ dependence evaluated using formula (48) (Fig. 5b, curve 1) does not vanish at $x = 0$ (at the boundary with the metal), nor do $\Psi(x)$ and $b_y(x)$ determining P_y . Other findings were that the $P_y(x)$ calculated via formula (48) for intermediate gap widths w (in particular, for $w = 10$ and $15.5 \mu\text{m}$) always has a maximum at the boundary $x = 0$, and that the total flux $\Pi(k_y)$ evaluated with formula (29) using these $P_y(x)$ does not change sign at dispersion extrema. For example, $\Pi(k_y)$ does not change sign in the range $0 < k_y < 2000 \text{ cm}^{-1}$ for $w = 10 \mu\text{m}$, even though a change of sign should be seen for $k_y \sim 570 \text{ cm}^{-1}$ as is the case for the similar $\Pi(k_y)$ dependence in Fig. 3a [$P_y(x)$ and $\Pi(k_y)$ dependences are not shown in the figures]. To avoid errors in our computations, we also calculated in the magnetostatic approximation the dependence $h_x(x)$ (Fig. 5b, curve 3), which proved to be identical to the similar dependence evaluated using Maxwell's equations (Fig. 4c, curve 3).

The above results indicate that formula (48) is inadequate for calculating MSW energy characteristics. Still, let us here briefly describe an experiment that provides further support for this conclusion. Details aside, the difference

⁴ Because b_y is imaginary, Fig. 5 shows the dependence $\operatorname{Re}(b_y(x))$.

between $P_y(x)$ calculated from formula (48) and Maxwell's equations lies in the fact that as the metal screen approaches the MSW-localizing surface of the ferrite plate (i.e., the surface whereat $P_y(x)$ has a maximum), calculations via formula (48) show that the wave remains localized near this surface, whereas computations based on Maxwell's equations give evidence that it changes localization by moving to the opposite surface of the plate. Thus, if an MSW localized near one of the surfaces of the ferrite plate encounters a metalized region on its way, then Maxwell's equations imply that, moving to the other surface, the wave will travel an additional distance equal approximately to the ferrite plate thickness, thus acquiring an additional phase incursion. If a grid of metallic strips is placed perpendicular to the wave's propagation direction and if a thicker plate is used, the additional phase incursion due to surface-to-surface 'transitions' will become measurably large.

Experiments that demonstrated this phase incursion are described in Ref. [17]. The basic idea of work [17] is to compare the results of two following experiments. In the first of them, the ferrite plate had exciting and receiving MSW transducers placed on its surface and what was measured was how the phase of the transmission coefficient changed between them as the grid of metallic strips was smoothly brought closer to the ferrite surface located between the transducers. The second experiment differed only in the employment of a metal screen rather than a grid of strips. Thus, if the MSW indeed made 'transitions' from one surface to the other, the phase incursions related to the length of each structure would be strongly different for these two experiments — as indeed they were found to be in Ref. [17] (so much different that they have even opposite signs) (see Ref. [17] for more details). Notice that if P_y were determined by formula (48), there would be only a slight phase incursion difference between these two experiments.

We have thus proved that formula (48) is incorrect and, hence, so are the results it produces.

The question, however, remains whether MSW energy characteristics can be calculated by treating the problem in the magnetostatic approximation. The answer is YES, provided only that calculations are made with formula (16) which, for our problem, reduces to formula (17). As already noted, the SHF component h_x entering into formula (17) is virtually the same whether calculated magnetostatically (Fig. 5b, curve 3) or using Maxwell's equations (Fig. 4c, curve 3). What remains to be done is to find the SHF field component e_z that enters into formula (17). Clearly, because the first equation of system (4) assumed the form $\text{rot } \mathbf{h} = 0$, it is of no use for finding e_z , leaving the second equation in the system for this purpose. For the ferrite layer, for example, noting the z -uniformity ($\partial/\partial z \equiv 0$), we obtain the following equation [analogous to the second equation in system (5)]:

$$\frac{\partial e_{2z}}{\partial y} = -i \frac{\omega}{c} (\mu h_{2x} + i v h_{2y}) = -i \frac{\omega}{c} b_{2x}. \quad (49)$$

Noting that all MSW characteristics, including the e_z component, vary with y as $\exp(-ik_y y)$, equation (49) is readily integrated to yield

$$e_{2z} = \frac{k_0}{k_y} b_{2x} = \frac{k_0}{k_y} (\mu h_{2x} + i v h_{2y}). \quad (50)$$

For SHF components e_{jz} in a vacuum ($j = 1, 3$), we obtain by analogy that

$$e_{jz} = \frac{k_0}{k_y} b_{jx} = \frac{k_0}{k_y} h_{jx}. \quad (51)$$

Taking account of Eqns (50) and (51), expression (17) for P_{jy} may be rewritten as

$$P_{jy} = \frac{\omega}{8\pi k_y} \text{Re}(b_{jx} h_{jx}^*) = \frac{V_{\text{ph}}}{8\pi} \text{Re}(b_{jx} h_{jx}^*), \quad (52)$$

where V_{ph} is the MSW phase velocity in an FDM structure.

The curve $P_{jy}(x)$ calculated using formula (52) for various values of w is identical to its analog in Fig. 4 calculated from Maxwell's equations. That this should be so becomes obvious when one compares formulas (17) and (52): both e_z and b_x vanish at the metal surface, and this is exactly what determines the behavior of $P_y(x)$ [it is also worth noting that the calculated results from formula (48) are not identical to those from formulas (17) and (52) because neither Ψ nor b_y entering into formula (48) is equal to zero at the metal surface]. It is also clear that the total flux Π and partial fluxes Π_j calculated in accordance with formula (29) based on relationship (52) will be nearly identical to their counterparts calculated using Maxwell's equations, with the accuracy of this coincidence (as with other magnetostatic calculations) increasing with a decrease in the ratio k_0/k_y (see Ref. [18] for more details).

We have thus shown that when applying the magnetostatic approximation, the Poynting vector should also be calculated by formula (16), with the necessary components of the field \mathbf{e} determined from the second equation of the system (4). The only thing to remember is that, because in such a treatment the first equation in system (4) takes the form $\text{rot } \mathbf{h} = 0$, the permittivities of the ferrite and its surrounding dielectrics will be left out of account (which can be of little significance if they are small), so one should use Maxwell's equations if accurate computations are needed. Notice also that formula (52) is not universal: it holds only for the special case of an MSW propagating perpendicular to a uniform magnetic field \mathbf{H}_0 in a tangentially magnetized structure (with one or two metal screens or 'magnetic walls' [22]). In addition, one should not, when treating a problem magnetostatically, identify $\Psi(x)$, the magnetic potential distribution in the cross section of the structure, with $P_y(x)$, the MSW energy density distribution (such an analogy is often drawn in ferrite structure studies): from a comparison of Fig. 4c and Fig. 5b it is seen that the distributions $\Psi(x)$ and $P_y(x)$ may differ considerably.

6. The physical meaning of total and partial power fluxes

Let us return, however, to the results obtained in Section 4. By looking at how the total (Π) and partial (Π_j) fluxes vary as a function of the propagation constant k_y , it should be pointed out that the Π_1 and Π_3 fluxes in vacuum are always positive, whereas the Π_2 flux in the ferrite plate may be positive or negative, depending on the particular range of k_y values (see Fig. 3). The question that often arises here is, does this mean that the latter case produces a situation in which the energy transfer direction is different for vacuum and ferrite. Were such a change observed for one flux in a vacuum, it would be possible to establish experimentally when and where the

energy is transferred there, whereas such measurements are impossible within the ferrite plate.

We will therefore try to use logical reasoning to find the answer. We begin by noting that when calculating the total flux Π , the only reason why the integral over x was written as the sum of three integrals was a convenience. More than three would do as well. For example, let us divide the integral over the ferrite layer from $-s$ to 0 into two regions, from $-s$ to $-x_0$ and from $-x_0$ to 0 , and let $x = -x_0$ correspond to that plane in the ferrite layer where $P_y(x)$ passes through zero (such a point, $x = -x_0$, can be seen in Figs 4a and b). Integrating in this new way, for example, for the case in Fig. 4a and reasoning about the signs of the new partial fluxes Π_{21} and Π_{22} , is it valid to conclude that it is not the flux in the whole of the ferrite plate but only the Π_{22} flux (obtained by integrating from $-x_0$ to 0) that is negative? Or can the limits of integration in the ferrite layer in, for example, the case of Fig. 4b be chosen such that the integral over most of the ferrite plate thickness is zero, but will this imply that the energy flux is not at all present in that part of the plate?

Thus, it is easily seen that when determining the wave energy propagation direction, only the magnitude and sign of the integral as a whole or, in other words, of the total flux Π are physically meaningful (irrespective of the number of regions into which the integration is divided). Clearly, this general conclusion applies not only to an MSW in an FDM structure but also to waves of another nature propagating in any other structure.

Another often asked question may be stated as follows: Is there any physical meaning to partial fluxes? A possible answer is this: the physical meaning of partial fluxes is similar to their mathematical meaning in the sense that it is determined by the proportion of wave energy in a given region of integration; however, to avoid errors in choosing arbitrary (although possibly convenient) integration intervals (as in Fig. 4b, where the integral over most of the ferrite plate thickness may prove to be nearly zero), these intervals should be taken sufficiently small or, one can say, it is more convenient in this context to analyze the behavior of the original (integrand) flux density P in the cross section of the structure. It is this dependence which provides complete insight into how the time-averaged energy flux density is distributed in a structure (medium). Still, the case in which the limits of integration for calculating the total flux coincide with the boundaries of a component media should be given special consideration. In this case, if the Poynting vector is positive (or negative) throughout the range of integration, then knowing partial fluxes means knowing which proportion of power is localized in the corresponding medium (i.e., layer of the structure).

7. Conclusion

The energy characteristics of a dipole spin wave whose dispersion curve in a ferrite–dielectric–metal structure possesses extrema have been calculated and analyzed to demonstrate the manifestation near these points of fundamental relationships among such wave parameters as the propagation constant, phase velocity, group velocity, Poynting vector, and electromagnetic energy flux. It is shown, in particular, that in this structure the total power flux Π and the dispersion curve $f(k_y)$ change in a related way: for those values of the propagation constant k_y for which $f(k_y)$ has an extremum, the flux Π is zero, with the flux Π and the phase

velocity of the wave (the propagation constant) having the same sign for those intervals of k_y where the wave is forward (i.e., where the dot product of the wave vector and the group velocity is positive, $\mathbf{k}_y \mathbf{V} = \mathbf{k}_y \partial \omega / \partial \mathbf{k}_y > 0$), and having opposite signs for those intervals of k_y where the wave is backward (i.e., where $\mathbf{k}_y \mathbf{V} = \mathbf{k}_y \partial \omega / \partial \mathbf{k}_y < 0$). The validity of these findings is confirmed by previous experimental work.

The study of these relationships using Maxwell's equations shows that calculating the Poynting vector \mathbf{P} in a ferrite structure using the formula $\mathbf{P} = -\omega \operatorname{Re} (i \Psi^* \mathbf{b}) / 8\pi$ (where Ψ is the magnetic potential, and \mathbf{b} is the magnetic induction vector) obtained in earlier work [4, § 5.1; 6, § 6.1; 9, 10] leads to incorrect results because the relationships described above do not manifest themselves in this case. In describing dipole spin waves in the magnetostatic approximation, one should calculate the Poynting vector by the well-known formula $\mathbf{P} = c \operatorname{Re} [\mathbf{e} \mathbf{h}^*] / 8\pi$, determining the SHF field \mathbf{e} from Maxwell's equation $\operatorname{rot} \mathbf{e} = -i\omega \mathbf{b} / c$.

The work was supported in part by the Higher School Research Potential Development grant No. 2. 1. 1 /1081.

References

1. Crawford F S (Jr.) *Berkeley Physics Course* Vol. 3 *Waves* (New York: McGraw-Hill, 1968) [Translated into Russian (Moscow: Nauka, 1974)]
2. Felsen L B, Marcuvitz N *Radiation and Scattering of Waves* (Englewood Cliffs, NJ: Prentice-Hall, 1973) [Translated into Russian (Moscow: Mir, 1978)]
3. Damon R W, Eshbach J R *J. Phys. Chem. Solids* **19** 308 (1961)
4. Vashkovsky A V, Stal'makhov V S, Sharaevskii Yu P *Magnitostatische Volny v Elektronike Sverkhvysokikh Chastot* (Magnetostatic Waves in Super-High-Frequency Electronics) (Saratov: Saratov Univ. Publ., 1993)
5. Gurevich A G, Melkov G A *Magnitnye Kolebaniya i Volny* (Magnetization Oscillations and Waves) (Moscow: Nauka, 1994) [Translated into English (Boca Raton: CRC Press, 1996)]
6. Stancil D D, Prabhakar A *Spin Waves: Theory and Applications* (New York: Springer Science + Business Media, 2009)
7. Yukawa T et al. *Jpn. J. Appl. Phys.* **16** 2187 (1977)
8. Zubkov V I, Shcheglov V I *Radiotekh. Elektron.* **42** 1114 (1997) [*J. Commun. Technol. Electron.* **42** 1036 (1997)]
9. Gupta S S, Srivastava N C *J. Appl. Phys.* **50** 6697 (1979)
10. Gupta S *IEEE Trans. Magnetics* **18** 1639 (1982)
11. Vendik O G, Kalinikos B A, Miteva S I *Izv. Vyssh. Uchebn. Zaved. Radioelektron.* **24** (9) 52 (1981)
12. Shchuchinskii A G *Radiotekh. Elektron.* **29** 1700 (1984)
13. Golovko Ya D et al. *Fiz. Tverd. Tela* **29** 3492 (1987) [*Sov. Phys. Solid State* **29** 2004 (1987)]
14. Danilov V V, Zavislyak I V, Balinskii M G *Spinvolnovaya Elektrodinamika* (Spin Wave Electrodynamics) (Kiev: Lybid', 1991)
15. Vashkovskii A V, Lokk E G *Radiotekh. Elektron.* **46** 729 (2001) [*J. Commun. Technol. Electron.* **46** 674 (2001)]
16. Vashkovskii A V, Lokk E G *Radiotekh. Elektron.* **47** 97 (2002) [*J. Commun. Technol. Electron.* **47** 87 (2002)]
17. Lokk E G *Radiotekh. Elektron.* **50** 74 (2005) [*J. Commun. Technol. Electron.* **50** 67 (2005)]
18. Vashkovsky A V, Lock E H *Usp. Fiz. Nauk* **176** 557 (2006) [*Phys. Usp.* **49** 537 (2006)]
19. Shevchenko V V *Usp. Fiz. Nauk* **177** 301 (2007) [*Phys. Usp.* **50** 287 (2007)]
20. Vashkovskii A V, Lokk E H *Usp. Fiz. Nauk* **174** 657 (2004) [*Phys. Usp.* **47** 601 (2004)]
21. Tamir T, Oliner A A *Proc. IEEE* **51** 317 (1963)
22. Lokk E G *Radiotekh. Elektron.* **52** 202 (2007) [*J. Commun. Technol. Electron.* **52** 189 (2007)]